03,15

Investigation of electrical resistance and thermal emf of a single crystal of samarium monoselenide under temperature cycling in the range of 320−800 K

© N.N. Stepanov, G.A. Kamenskaya, S.V. Novikov

Ioffe Institute,
St. Petersburg, Russia

E-mail: stnick@mail.ioffe.ru

Received February 27, 2024
Revised February 27, 2024
Accepted March 26, 2024.

A study of the temperature dependences of the specific electrical resistance ρ and thermal S of a single crystal of samarium monoselenide SmSe in five cycles in the range 320−800 K. After the third measurement cycle of the single crystal, its temperature annealing was performed in an ampoule pumped to 10^{-7} MPa at $T = 675$ K for 6 hours. Upon completion of the annealing procedure, two cycles of measurements were performed on the sample. It has been established that cyclic temperature action on the SmSe single crystal, as well as temperature annealing, lead to the appearance of hysteresis on the dependences $\ln[\rho(10^3/T)]$ and $S(T)$. The analysis of the discovered patterns in the behavior of ρ and S allowed us to make an assumption about the significant influence of the processes of occurrence and destruction of the exciton spectrum under the influence of temperature changes on the processes of electrical transfer in SmSe

Keywords: samarium monoselenide, thermal EMF, specific electrical resistance, excitons.

DOI: 10.61011/PSS.2024.05.58493.37

1. Introduction

Samarium monoselenide SmSe is one of the representatives of the family of semiconductor rare earth (REE) monochalcogenides that have been studied over the years. These compounds have a set of unique physical and chemical properties, that, in particular, include structural and electronic phase transformations, and features of electrotransport processes in a wide pressure and temperature region. By a number of electrophysical and thermodynamic properties (see, for example, [1–3]), SmSe may be treated as a promising material for sensitive elements of high-temperature strain gage and pressure sensors where it is used both a an individual compound and as part of solid solutions.

This paper describes the findings of the experimental investigations of resistance and thermal emf behavior of samarium monoselenide in the temperature range of 320−800 K. The experimental data analysis suggests a number of features of the transport properties of charge carriers in SmSe within the specified temperature range.

2. Experiment procedure

Stoichiometric SmS single-crystals were prepared using technique [4]. A $\sim 12 \times 5 \times 2$ mm test sample was chipped out from a synthesized ingot on [100] cleavage plane of the material.

According to the X-ray diffraction analysis, SmSe crystal FCC lattice constant (space group $Fm\bar{3}m$) of the test sample was equal to $a_{\mathrm{SmSe}} = 6.196$ Å that was typical for SmSe at $T = 300$ K and atmospheric pressure of $P = 0.1$ MPa; the X-ray coherent scattering region (CSR) was $L_{\mathrm{SmSe}} \sim 2500$ Å, which corresponds to a quite well-formed single-crystal. Specific resistance and thermal emf of SmSe in the specified conditions were equal to $\rho \approx 1500\,\Omega\cdot$cm and $S \approx -700\,\mu$V/K, respectively.

Temperature dependences of resistivity ρ and thermal emfS of SmS single-crystals in the region from 320 to 800 K were examined on the setup described in detail in [5]. A total of five measurements of ρ and S were conducted in temperature cycling condition („heating-cooling“).

After three measurement cycles, the sample was subjected to annealing at $T \sim 675$ K during 6 h in a quartz tube evacuated to 10^{-7} MPa and sealed. After the heat treatment, another two measurements of ρ and S were performed.

Temperature trend of the resistivity R of SmS single-crystal was studied by the four-probe AC method using spring-loaded platinum contacts. temperature and temperature gradient along the maximum dimension of the sample were measured using two Pt-Pt/Rh thermocouples. Thermal emf of the test material was calculated considering the thermal emf of the thermocouple.

3. Measurement data

Figure 1 shows the dependences of log resistance of SmS single-crystal on the reciprocal temperature with weight coefficient 10^3 for five thermal measurement cycles (thermal cycles). After the first three thermal cycles the test

SmSe sample underwent an additional vacuum annealing (see above) and measurements were continued.

Analysis of the obtained data identifies features in the form of bends on $\ln[\rho(10^3/T)]$ curves of SmSe in a temperature region near 615 K and their minor deviations from the initial values in various temperature cycles. The first measurement cycle shows the largest difference in $\ln[\rho(10^3/T)]$ values of direct and reverse temperature trends that is particularly pronounced within 500–700 K (see the Detail in Figure 1). In the next measurement cycles, such deviations are reduced negligibly.

To understand the changes in electrotransport processes in SmSe under cyclic temperature loads, Figure 2 shows dependences of specific resistance log function deviation $\Delta\ln[\rho(10^3/T)]$ of the sample on reciprocal temperature (with weight coefficient 10^3) about the line segments connecting the points on the measurement range boundaries of the former. These dependences were calculated in each experiment separately for heating and cooling processes (i.e. for each half cycle) of SmSe sample.

$\Delta\ln[\rho(10^3/T)]$ curves are shown in Figure 2. Analysis of these dependences shows that they have features in the form of bends in the range of 550–720 K and hysteresis when the test sample passes this temperature range in the thermal cycle. The hysteresis amplitude decreases from the first to the third thermal cycle. After annealing of the sample, the hysteresis amplitudes even increased a little in next two thermal cycles, but their decreasing effect during cyclic heating remains. Moreover, on $\Delta\ln[\rho(10^3/T)]$ of the first heating sample after annealing a feature in the form of additional bend was detected at $T \approx 670$ K that

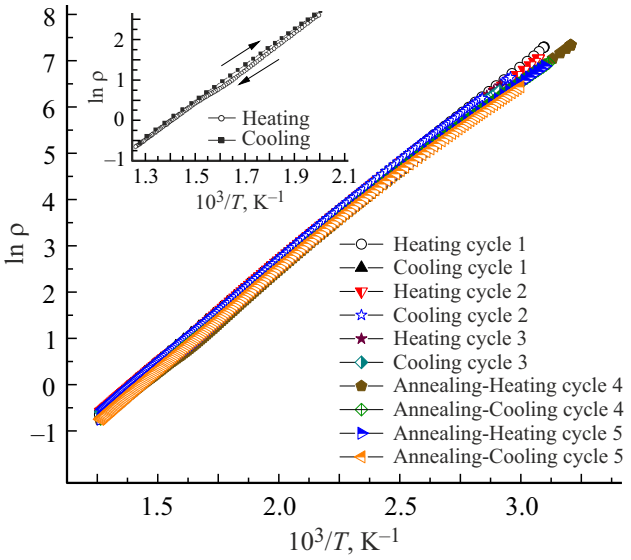

Figure 1. Dependences of specific resistance log $\ln[\rho(10^3/T)]$ of the SmSe single-crystal on reciprocal temperature for five measurement cycles — „heating –cooling". *1* — thermal cycles 1–3; *2* — thermal cycles 4, 5 (after sample annealing); *a* — fragment of $\ln[\rho(10^3/T)]$ in the first temperature cycle.

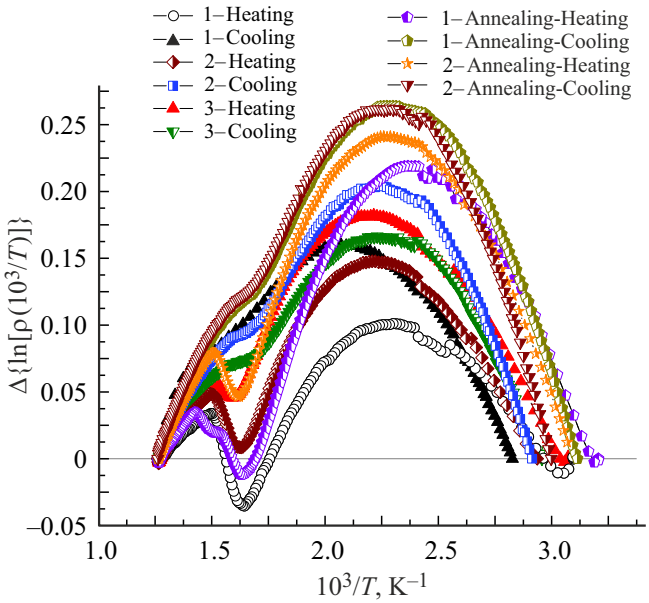

Figure 2. Curves of specific resistance deviation $\Delta\ln[\rho(10^3/T)]$ of the SmSe single-crystal vs. reciprocal temperature (with weight coefficient 10^3) for five thermal cycles.

had no equivalents in previous thermal cycles and shall be addressed separately.

The range of abnormal behavior of $\ln[\rho(10^3/T)]$ of SmSe may be more accurately defined by calculating their derivatives with respect to the reciprocal temperature and by plotting the temperature dependences of local activation energy $E_a(T)$ of free current carriers for each thermal cycle of the sample using the following relation: $\partial\{\ln[\rho(10^3/T)]\}/\partial(1/T) \cong k_B \cdot 10^3 \cdot E_a$, where k_B — is Boltzmann's constant (Figure 3). According to curves in Figure 3, the most pronounced anomalies in $E_a(T)$ behavior of SmSe are observed in the temperature range of 550–680 K. Activation energy $E_a \approx 0.36$ eV of SmSe obtained herein at $T = 300$ K approaches that defined before in [6] using pressure experiment data. temperature dependence of local $E_a(T)$ of SmSe demonstrates gradual growth in the temperature range from 350–500 K. Further temperature increase results in sudden drop of E_a by $\sim 35\%$ in the narrow temperature range $\Delta T \approx 50$ K (590–640 K), and then to the same fast increase by $\sim 26\%$ in the range from 640 to 670 K. Further temperature rise up to ~ 800 K again results in gradual increase of E_a, however, at a lower growth rate with respect to that observed at the initial temperature segment of $E_a(T)$ curve. The analysis of data shown in Figure 3 suggests that, when the sample temperature decreases, changes in the local activation energy of free current carriers have hysteresis with respect to the heating condition in each thermal cycle. In this case, $E_a(T)$ gradually decreases initially with temperature decreasing from 800 K to ~ 620 K, then grows by $\sim 8\%$ at 550–620 K, but, however, is still lower than the values observed at the specified temperatures in

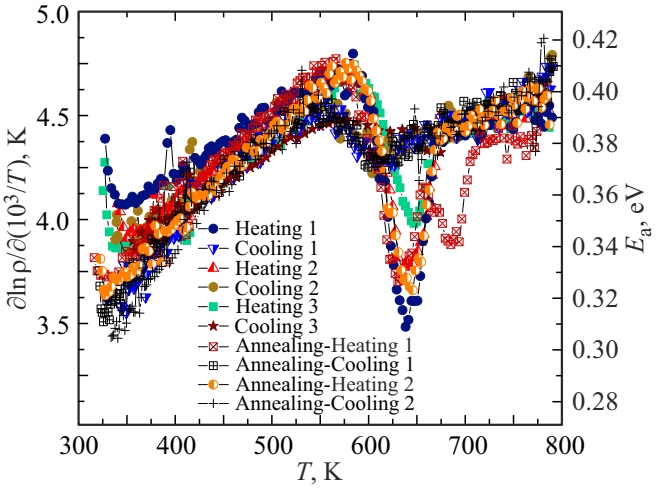

Figure 3. Temperature dependences of partial derivatives $\ln[\rho(10^3/T)]$ with respect to the reciprocal temperature (left-hand y scale) and local activation energies E_a of free current carriers in SmSe (right-hand x scale) for five measurement thermal cycles.

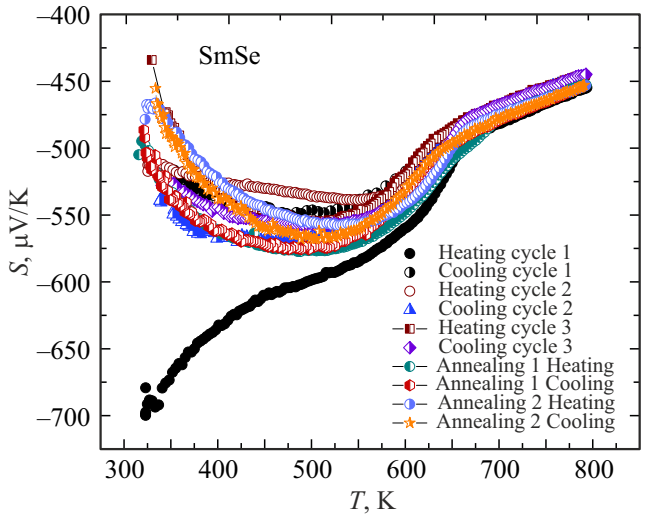

Figure 4. Dependences of thermal emf of the SmSe single-crystal on temperature obtained in five measurement thermal cycles.

the heating phase. Repeated temperature cycles reduce the hysteresis amplitude a little. $E_a(T)$ behavior in the fourth heating cycle features a non-monotonic transition to a straight high-temperature segment due to a peculiar pattern of $\ln[\rho(10^3/T)]$. This anomaly is not observed any longer in the fifth thermal cycle.

Additional information on the features of electric charge transport processes in the SmSe semiconductor phase may be obtained from the experimental temperature dependences of thermal emf $S(T)$ of the material shown in Figure 4.

What calls attention to itself is that there is considerable difference in the behavior of the temperature dependence of thermal emf of SmSe during the first heating of the sample from those obtained from measurements in the next temperature cycles. thermal emf of the SmSe sample smoothly grows with temperature rise throughout the test range of 320–800 K, and two inflection points may be noted on $S(T)$: at $T \approx 460$ K and $T \approx 670$ K (more accurately — 666 K) that are associated with variation of the electrotransport parameters in SmSe. Temperature range 615–670 K shows an increase of thermal emf growth rate that decreases suddenly during further heating of the sample. In the temperature region exceeding 670 K, $S(T)$ depends linearly on temperature up to 800 K and maintains such form almost without changes in the next measurement cycles. In the low-temperature region (320–570 K), repeated measurements of $S(T)$ in SmSe record significant change in its behavior on the temperature segment from 320 to 570 K. In the first cooling cycle, $S(T)$ starts growing with temperature decrease below 500 K. In the second heating cycle, $S(P)$ decreases as the temperature increases up to ~ 570 K, and then starts growing. When temperature decreases to ~ 520 K, the thermal emf decreases and starts growing with further cooling. In the third and next thermal cycles, S of SmSe generally repeats the behavior in the previous thermal cycles (excluding, certainly, the first heating of the sample).

4. Discussion

Findings of the study shall be discussed starting from Figure 5 that shows SmSe band spectrum diagram based on investigations [6–9],supplemented and partially updated with experimental facts established later and theoretical developments [3,10,11]. In the changed SmSe band structure diagram, inverted relative position of valleys of $5d_{t_{2g}}$- and $6s$-subbands of conduction band with respect to the initial position (see [9]) is assumed, presence of n-type and p-type levels and exciton states caused by $4f5d$-Coulomb interaction are considered [10]. According to theoretical opinions [11], the latter play a crucial role in phase transition in semiconductor SmS in uniform compression and in phase transitions at pressure in SmSe and SmTe [12].

Using the SmSe band structure diagram shown in Figure 5, electrotransport processes taking place in the compound during thermal cycling may be described as follows. When the SmSe sample is exposed to temperature up to 800 K, the following processes take place in its electronic subsystem: a) thermal activation of $4f^6$-electrons Sm^{2+} into bound (exciton) states $4f^5 5d_{ex}$ and into $6s$-$5d_{t_{2g}}$-subbands of the conduction band; b) p-type level filling by valence band electrons; c) partial compensation of acceptors by conductivity electrons, and the following may be suggested: d) disintegration of the exciton state system when some critical temperature of the sample is exceeded and subsequent transition of electrons previously bound in the excitons into the conduction band. As the sample cools down, its electronic subsystem gradually returns into the initial state, however this process has a feature. Thus, transition

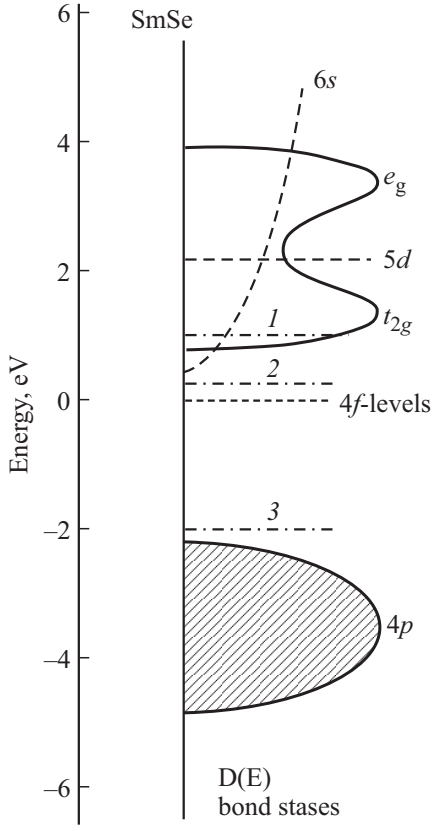

Figure 5. Band structure of SmSe semiconductor phase. *1* — positions of the first exciton level according to [10]; *2* — *n*-type level position according to the data obtained herein; *3* — *p*-type level position (not adequately defined).

of conductivity electrons from $5d_{t_{2g}}$-subband into bound $4f^5 5d_{\text{ex}}$-states (exciton spectrum restoration) may occur only as the sample temperature decreases by $\sim 20-25$ K (Figure 3), rather than in the disintegration temperature range of the latter. Therefore, hysteresis is observed on $E_a(T)$ in each thermal cycle. It should be also noted that sample temperature decrease shall ultimately result in exciton dissipation in SmSe due to the fact that they cannot occur as a result of termination of thermal activation of $4f^6$-electrons.

In support of the foregoing, we shall analyze the $\Delta\ln[\rho(10^3/T)]$ curves in Figure 2 that were calculated by subtracting the corresponding $\ln[\rho_i \exp(10^3 \cdot E_a^i/k_B T)]$ satisfying the following conditions from the dependences $\ln\rho(10^3/T^i)|_{i=1-10}$ plotted using the experimental data for each i-th measurement half cycle: $\ln\rho(10^3/T^i_{\text{i,f}}) = \ln[\rho_i \exp(10^3 \cdot E_a^i/k_B T^i_{\text{i,f}})]$; where $\partial\rho_i \partial T = 0$, T_{i}^i and T_{f}^i — are initial and final temperatures of the i-th half cycle; $E_a^i = \text{const}(T)$ are constants measured in energy units. E_a^i values correspond to the averaged local activation energies $\bar{E}_a$ of in i-half cycles in the reciprocal temperature range $\Delta(1/T)_i = |1/T_{\text{i}} - 1/T_{\text{f}}|_i$.

It should be noted that the behavior of dependences $[\Delta\ln[\rho(10^3/T)]_{i=1-10}$ on the reciprocal temperature (with weight factor 10^3) cannot be consistently explained only by variation of free charge carrier scattering parameters as the temperature grows and $5d_{t_{2g}}$-subband of the conduction band of SmSe is integrated into the electrotransport processes. Actually, assuming the general provisions, optical phonons and charged defects — Sm^{3+} are the main scatterers of free charge carriers in SmSe at $320 < T < 800$ K: the former — because the experimental temperature range is much higher than the Debye temperature of SmSe $\theta_{\text{D}} = 206$ K [13], the latter — because their concentration is growing continuously as the sample is heated. In these conditions, mobility of the conductivity electrons decreases as the sample temperature grows, therefore, the related partial component ρ (and $\ln\rho$) shall increase as the latter generally decreases. Involvement of $5d_{t_{2g}}$-subband in the electrotransport shall result unambiguously in the deceleration of decrease of ρ (and $\ln\rho$) of SmSe with temperature growth because the density of states of electrons in it exceeds that in the 6*s*-subband. Obviously, both factors discussed above cannot explain not only the non-monotonic behavior of $[\Delta\ln[\rho(10^3/T)]_{i=1-10}$, but also the presence of hysteresis in thermal cycles.

Now consider possible results of the effect of cyclic temperature exposures within 320−800 K on the electronic state spectrum in SmSe. First, focus shall be made on the following: already during the first heating, annealing of the material sample occurs in SmSe involving variations of the stressed state of its crystal structure, concentration and distribution of dislocations, vacancies, impurities and interstitial inclusions. Second, there is reason to believe that there is partial evaporation from selenium crystal surface into the thermostat vacuum and, therefore, appearance of Se anion flow from within the material to compensate this decrease. Third, diffusion of light non-metals (carbon, oxygen, nitrogen) into the sample through its surface from the residual thermostat atmosphere. In other words, temperature exposure can distinctively restructure the SmSe electronic energy spectrum, including its exciton component. Thus, selenium vacancies formed within the sample may be partially filled with samarium cations that were previously located in the crystal lattice interstices. Transition of samarium cations from interstices to vacant positions in the selenium sublattice is energetically favorable, therefore, the ionization potential of $4f^6$-electrons of Sm^{2+} transferred to the anion positions in the regular crystal lattice grows. Then, diffusion of light non-metals (C, O, N) into the material results in firm chemical bonds between them and Sm cations, thus, blocking both activation from the last electrons into the conduction band [14] and formation of exciton pairs. Nevertheless, the experimental data show that the behavior of $\ln[\rho(10^3/T)]$ of SmSe in thermal cycles generally remains constant. Only the change in the trend of $S(T)$ near $T < 500$ K, observed after the first heating of the sample seems to be significant, however, the causes of this phenomenon are rather trivial and do not make fundamental changes in the SmSe charge carrier structure.

Let us turn to the analysis of the effects of exciton state spectrum formation and disintegration on electric and thermoelectric properties of SmSe. Sample heating, on the one hand, facilitates formation of excitons in SmSe at the initial stage, and, on the other hand, induces destruction of the latter as the temperature continues growing. Active generation of exciton pairs in SmSe starts at quite low temperatures probably within 370−400 K where instability of $[\Delta \ln[\rho(10^3/T)]_i$ behavior is observed (Figure 2). As the temperature grows (up to a particular limit), the exciton concentration in the sample increases. The generated exciton states play a role of electron traps [15] that reduce the rate of decrease of ρ of SmSe with temperature growth. However, as soon as during heating up to $T \sim 560-580$ K, exciton disintegration process starts developing in the sample as it appears from formation of smoothed peaks on $E_a^i(T)$ (Figure 3). Boundaries of high-temperature exciton state instability regions in SmSe are defined from $E_a^i(T)$ separately for each cycle. According to the acquired data, exciton system disintegration starts when the sample achieves ~ 590 K, and ends at ~ 640 K for the first three and the fifth thermal cycle. Destruction of the exciton state system induces electron transition not only into 6*s*-subband, but also into $5d_{t_{2g}}$-subband of the conduction band with a „heavy“ effective carrier mass resulting in (as mentioned above) deceleration of $E_a(T)$ growth at $T \geq 650$ K.

Behavior of $\Delta \ln[\rho(10^3/T)]$ and $E_a(T)$ obtained in the fourth thermal cycle during heating of the heat treated SmSe sample indicates a complex structure of the exciton spectrum generated by annealing. There is good reason to believe that some part of Sm cations in the sample is located in the vacancies of the crystal anion sublattice forming a system of „deep“ n-type levels and, accordingly, a related exciton spectrum subsystem of the compound, while the other part remains in interstices. Owing to this, the SmSe exciton structure in the high-temperature region disintegrates stage-by-stage and this fact is exhibited most distinctly on the corresponding dependence $E_a(T)$.

Let us analyze the thermal emf — temperature dependences of SmSe. $S(T)$ behavior in the first cycle during heating up to 460 K is typical for a partly compensated *n*-type semiconductor with dominating transport over 6*s*-subband of the conduction band. At temperatures not exceeding the temperature mentioned above, the effect of hole conductivity may be neglected and conductivity in SmSe may be treated as purely electronic. Considerable change in the thermal emf behavior at $T < 500$ K after the first heating of the sample may be explained by the fact that some cations that had been previously located in interstices moved to vacant positions in the anion sublattice under the temperature exposure. As a result, the activation energy of their $4f$-electrons has increased, thus, the electron concentration has decreased in the conduction band and the effect of charge transport over the SmSe valence band on the magnitude of the sample's thermal emf has appeared.

Figure 6 shows polynomial approximation lines of derivative $\partial S/\partial T$ for all 5 thermal cycles. According to the first of

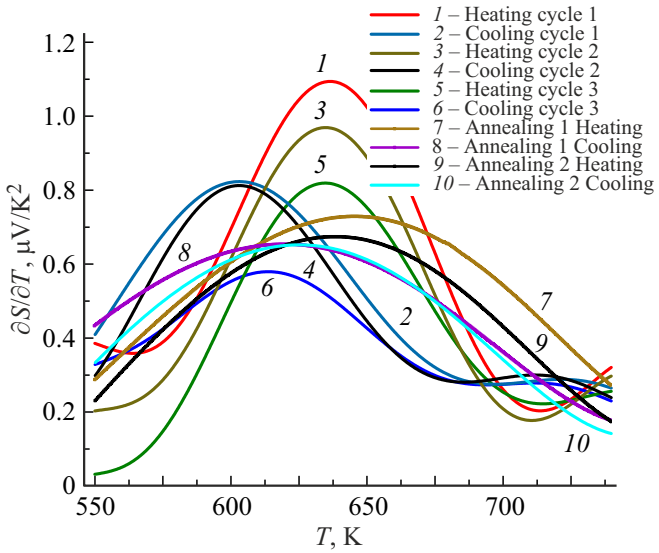

Figure 6. Polynomial approximation lines of $\partial S/\partial T$ of SmSe single-crystal for five thermal cycles.

the curves shown in Figure 6, $S(T)$ achieves the highest growth rate at $T \approx 640$ K, i.e. in the point where the valley of the temperature dependence of the local activation energy $E_a(T)$ is observed. With further temperature growth, the rate of change of $S(T)$ decelerates and transits to a smooth rise within 670−800 K. By the type of dependence, taking into account the SmSe band structure, it is suggested that two subbands — 6*s*- and $5d_{t_{2g}}$-, with „light“ (6*s*) and „heavy“ (5*d*) effective carrier mass are involved in the high-temperature electrotransport process. Since, during heating, the thermal emf behavior in the high-temperature region (670−800 K) almost coincides with that during heating, it can be noted that annealing has almost no effect on the SmSe conduction band spectrum properties. $S(T)$ behavior in SmSe during the first temperature decrease and during next thermal cycles is defined by the current carrier electron spectrum in the crystal that has been already changed after annealing (with slight variations in each cycle). Due to the abovementioned causes, temperatures of $\partial S(T)/\partial T$ peaks in SmSe in thermal cycles are not the same: during heating, they are higher ($T_{\max} \sim 630-640$ K) than during cooling ($T_{\max} \sim 604-614$ K), i. e. hysteresis is observed.

5. Conclusion

The study describes the findings of experimental studies of temperature dependences of specific resistance ρ and thermal emf S of SmSe single-crystal within 320−800 K in five temperature measurement cycles. After the first three cycles, the sample was annealed and the experiment was continued. Considerable impact induced by temperature exposure and annealing of the sample on the electrotransport parameters in the SmSe single-crystal was detected. To explain the observed effects, a qualitative model is

proposed for exciton state spectrum restructuring in SmSe when it is exposed to temperature: appearance of excitons at the initial sample heating stage, subsequent dissipation of exciton states when the critical temperature of ~ 590 K is exceeded in the material, exciton spectrum restoration during adequate cooling of the sample (by ~ 30 K below the specified temperature) and its further disintegration at $T < 370$ K.

Conflict of interest

The authors declare that they have no conflict of interest.

References

[1] V.V. Kaminsky, N.V. Shrenkova. FTP, **53**, 158 (2019). (in Russian).
[2] A.V. Golubkov, E.V. Goncharova, V.P. Zhuze, G.M. Loginov, V.M. Sergeeva, I.A. Smirnov. V kn.: Fizicheskie svoistva khal'kogenidov redkozemel'nykh elementov'/Pod.red. V.P. Zhuze. Nauka, L., (1973). Gl. 2. P. 58. (in Russian).
[3] S.G. Grebinsky, V.V. Kaminsky, N.N. Stepanov, I.A. Smirnov, A.V. Golubkov. FTT **25**, 151 (1983). (in Russian).
[4] A.V. Golubkov, V.M. Sergeeva. Fizika i khimiya redkozemelnykh poluprovodnikov (Khimiya itekhnologiya). Preprint UNTs AN SSSR, Sverdlovsk (1977). S. 28. (in Russian).
[5] A.T. Burkov, A.I. Fedotov, A.A. Kas'yanov, R.I. Panteleev, T. Nakama. Nauch.-tekhn. vestn. informatsionnykh tekhnologij, mekhaniki i optiki, **15**, *2*, 173 (2015). (in Russian).
[6] A.G. Gavrilyuk, V.A. Sidorov, I.A. Smirnov, N.N. Stepanov, L.G. Khvostantsev, O.B. Tsiok, A.B. Barabanov, A.V. Golubkov. FTT **28**, 2135 (1986). (in Russian).
[7] G.H. Dieke. Sprectra and Energy Levels of Rare Earth Ions in Crystals. Interscience Publ. (1968).
[8] M.I. Nathan, F. Holtzberg, J.E. Smith, Jr., J.B. Torrance, J.C. Tsang. Phys. Rev. Lett. **34**, 467 (1975).
[9] B. Batlogg, E. Kaldis, A. Schlegel, P. Wachter. Phys. Rev. B **14**, 5503 (1976).
[10] I.A. Smirnov, V.S. Oskotsky. UFN, **124**, 241 (1978). (in Russian).
[11] K.A. Kikoin. ZhETF **85**, 1000 (1983). (in Russian).
[12] A. Jayaraman, V. Narayanamurti, E. Bucher, R.G. Maines. Phys. Rev. Lett. **25**, 1430 (1970).
[13] A.V. Golubkov, E.V. Goncharova, V.P. Zhuze, G.M. Loginov, V.M. Sergeeva, I.A. Smirnov. V kn.: Fizicheskie svoistva khal'kogenidov redkozemel'nykh elementov /Pod. red. V.P. Zhuze. Nauka, L., (1973). Gl. 3 S. 132. (in Russian).
[14] L.N. Vasilyev, V.V. Kaminsky, M.V. Romanova, N.V. Sharenkova, A.. Golubkov. FTT **48**, *10*, 1777 (2006). (in Russian).
[15] V.A. Sidorov, N.N. Stepanov, L.G. khvostantsev, O.B. Tsiok, A.V. Golubkov, V.S. Oskotsky, I.A. Smirnov. V sb.: Fizika i khimiya redkozemelnykh poluprovodnikov / Pod. red. K.E. Mironova. Nauka, Novosibirsk (1990). S. 176. (in Russian).

Translated by E.Ilinskaya